

# Back-Illuminated Dye-Sensitized Solar Cell Flexible Photoanode on Titanium Foil

S. Shaban<sup>1\*</sup>, S. Shafie<sup>2</sup>, S.S. Pandey<sup>3</sup>, M.Q. Lokman<sup>4</sup>, F. Ahmad<sup>4</sup>, M.N. Hamidon<sup>1,2</sup>, and N.F.M. Sharif<sup>2</sup>

<sup>1</sup>*Institute of Advanced Technology, Universiti Putra Malaysia, 43400 Serdang, Selangor Darul Ehsan*

<sup>2</sup>*Faculty of Engineering, Universiti Putra Malaysia, 43400 Serdang, Selangor Darul Ehsan*

<sup>3</sup>*Graduate School of Life Science and Systems Engineering, Kyushu Institute of Technology, Wakamatsu, Kitakyushu, Fukuoka 808-0196, Japan*

<sup>4</sup>*Malaysia-Japan International Institute of Technology, Universiti Teknologi Malaysia, 54100 Kuala Lumpur*

This paper reports the preparation and performance analysis on dye-sensitized solar cells (DSSC) using titanium (Ti) foil as flexible photoanode for back-illuminated measurement. Performance differences were also carried with the fluorine-doped tin oxide (FTO) glass photoanode using the back and front-illuminated technique. The hydrogen peroxide (H<sub>2</sub>O<sub>2</sub>) treated Ti foil surface was applied and the doctor blade method was used for deposition on photoanode during the process of fabrication. Surface morphology of the treated Ti Foil with H<sub>2</sub>O<sub>2</sub> shows the formation of TiO<sub>2</sub> nanostructure which results in significant attachment of TiO<sub>2</sub> layer on Ti Foil. The results on measurement show that the fabricated flexible photoanode DSSC has an efficiency of power conversion at 1.00% under 1.5 A.M solar radiation by using back-illuminated while DSSC with solid-state glass photoanode has an efficiency power conversion at 0.53% (back-illuminated) and 2.22% (front-illuminated). However, the flexible photoanode DSSC has better power conversion efficiency than the solid-state glass photoanode DSSC under the condition of back-illumination. It is lower in result comparatively with front illumination DSSC due to the coated of platinum at the counter electrode that reflects light partially, while electrolyte iodine absorbs some photons and effects on DSSC performance.

**Keywords:** DSSC; Solar Cell; Ti Foil; Back-Illumination; Flexible Photoanode

## I. INTRODUCTION

Renewable energy nowadays is experiencing an increment of worldwide attention due to various profits in an extended period as it is inexpensive and eco-friendly. Commonly, renewable energy was originated from resources which are renewable such as; hydro, wind, solar, and geothermal. Few supereminent among all and large scale utilization which started from small scale systems such as photovoltaic power station and the digital solar calculator, is the solar energy. Electricity is converted from photon to direct current via solar

modules. The core of the sun emits nuclear fusion power committed to form the energy (Ellabban *et al.*, 2014).

There are several peer groups of photovoltaic technologies in solar energy. First generation of the photovoltaic mono-crystalline also known as polycrystalline silicon, demonstrates typical efficiency of 15% to 25 % (Sharma *et al.*, 2015). The good performance of this solar cell technology as well as high stability is the benefit of this PV Cell (Kranz *et al.*, 2015). However, lots of energy and expensive production cost is needed. Thin-film solar cells are the next group using cadmium telluride (CdTe), copper indium gallium selenide (CIGS) including

---

\*Corresponding author's e-mail: surayashaban@gmail.com

amorphous silicon (a-Si), where efficiency at 10% to 15% was achieved (Ferekides *et al.*, 1994). It also lowers the fabrication cost since it avoids the usage of silicon wafer processes. High-temperature treatment and vacuum involvement during production is associated with large energy consumption. Furthermore, low sufficient source of CdTe on second generation solar cells for the demand and this is the cause of the price restrain factor. The thin-film CdTe solar cell production must be handled carefully as it is toxic for human beings (Fthenakis *et al.*, 1999). Third generation solar cells are mostly polymers, and organic, consisting of tiny molecules. It contributes to a lower cost although its efficiency could go up to 20%. Perovskite solar cell is currently under investigation with great potential with efficiencies recorded at 20% on very small areas (Conibeer *et al.*, 2016). Despite that, perovskite vulnerability suffers from unstable processes, considering it should be fabricated in a strict, uncontaminated area with humidity temperature control.

Dye-Sensitized Solar Cell (DSSC) are in the third generation PV group that exchanges light energy to a voltaic energy constructed on the dye molecules absorption in wide-bandgap of a semiconductor film. Dye-sensitized Solar Cell received global attention due to its increasing energy conversion efficiency at 11.9% and it also has moderate cost of production (Tsai *et al.*, 2013; Buda *et al.*, 2017; Buda *et al.*, 2017). Important components for common DSSCs are wide band-gap semiconductor, synthetic sensitizer to act as a photoanode, catalyst, redox couple, and mechanical support. The photoanode is normally a dye particle coated together with the nanopore metal oxide semiconductor film deposited on the TCO glass substrate as the working electrode. The platinum (Pt) catalyst deposited on TCO substrate acts as the counter electrode and redox couple mediator is the iodide-triiodide ( $I^-/I_3^-$ ) electrolyte (Fan *et al.*, 2013).

Metal oxide semiconductor comprises of  $TiO_2$ , ZnO and SnO. The semiconductor is engaged as a light absorber and photo-induced charge separation transport are different the functioning of a DSSC. In an ordinary DSSC, light is absorbed by a molecule in a synthetic dye sensitizer familiarly known as N719, which conducts to the n-type semiconductor wide band-gap surface (Cavallo *et al.*, 2017). The dye sensitizer is DSSC photographic component as when it is sensitized by any visible light, it will be converted to electricity. The dye excites electrons from the ground state and then injects the excited electron to the nanocrystalline  $TiO_2$  semiconductor after seizing photons from any visible source. TCO glass with Pt coating counter electrode performs the catalytic activity of

$I^-/I_3^-$  reduction (Tsekouras *et al.*, 2008). Electrolyte redox mediators assist to connect and reconstruct the oxidized dye. Most redox mediators with slow recombination rate with the injected electrons chosen are the  $I^-/I_3^-$  couple (Gu *et al.*, 2017). The electrolyte closes the circuit as the electrons yield to the sensitizer. These electrons create energy and gather them to the load appliances. Some alteration made to the common DSSC with regards to the substrates are flexible DSSC. As it has excellent electrical conductivity, metal materials were chosen. Besides, its bendability and pliable, at high thermal treatment stability matched to the plastic, surface resistivity lower than indium tin oxide/polyethylene tetrathylate (ITO/PET), plus as inexpensive production cost puts metal a good substitute (Lin *et al.*, 2010). The implementation of metal as a working electrode for DSSC substrates could minimize the internal resistance on substrates yet helps the productivity of the solar cell and mark down the cost of the devices. Various metals carried out nowadays as substitution include W, StSt, Ni, Ti, Co, Pt, Cu, Al, and Zn (Wu *et al.*, 2017).

The preliminary article studied such  $H_2O_2$  treatment on Ti foil photoanode is an excellent example. This is because the  $H_2O_2$ -treated Ti foil shows a high device area due to the networked  $TiO_2$  nanosheets formed, which increases electrical correspondence between substrate and nanoparticles of  $TiO_2$  (Tsai *et al.*, 2013). The oxidized Ti foil layer surface property and treatments have been established to profoundly control surface adhesion and ideal electrical contact of Ti-wires coated  $TiO_2$  (Kapil *et al.*, 2014).

This paper discusses the surface treatment of Ti Foil and deposition method of  $TiO_2$  paste on Ti Foil as flexible photoanode for back-illuminated DSSC. This is very important because a suitable method is capable to make  $TiO_2$  layer properly attached to Ti Foil so it would not crack after annealing and detached while immersed in the dye. The step-by-step process in detail on flexible Ti foil fabrication as photoanode and the evaluation on the performance of the outcome are described in this paper.

## II. MATERIALS AND METHOD

### A. Material

The following materials were purchased from merchant

suppliers: pure metals (titanium (Ti) foil purity of 99.5%; The Nilaco Corporation), FTO conductive glass ( $> 83 \%$ ;  $< 15 \Omega/\text{sq}$ ; Zhuhai Kaivo Optoelectronic Technology Co., Ltd.), glacial acetic acid (ACS Analysis; 99.7%, J.T Baker), ethanol, ethyl alcohol, 2-propanol (Quality Reagent Chemical), chloroplatinic acid hexahydrate, titanium dioxide (TiO<sub>2</sub>) P25 anatase-nanopowder, hydrogen peroxide, H<sub>2</sub>O<sub>2</sub> (Sigma Aldrich), redox mediator iodine-based electrolyte (Solaronix). Di-tetrabutylammoniumcis-bis (isothiocyanato) bis (2,2-bipyridyl-4-dicarboxylato) ruthenium(II).

### B. Glass Substrates Preparation

Firstly, the FTO conductive glass with resistivity surface at  $15 \Omega/\text{sq}$  was chosen as the substrate, the glass slits to  $20 \text{ mm} \times 25 \text{ mm}$  with the usage of a Glass Cutter System (ZHKV-DT300) from the non-coated area. The slit glasses were cleaned with soap and sonicated to remove any surface contamination during slitting. Then, the glasses were placed in acetone and later the cleaning was repeated with ethanol and isopropanol and submitted to sonication for an additional 15 min respectively to eliminate organic contaminants. Finally, the excess fluid on glass substrates was dried after rinsing with de-ionized (DI) water deliberately.

### C. Flexible Photoanode Substrates Preparation

Next, the Ti foil was cut into  $20 \text{ mm} \times 25 \text{ mm}$ . Then the foil was cleaned with detergent, acetone, ethanol and isopropanol in 15 min respectively using ultra-sonicator. The Ti foil was then immersed into H<sub>2</sub>O<sub>2</sub> solution at (30 Wt. %, 20 mL) in a petri dish together with a magnetic bar depending on the diameter of the dish and spun 30 min with speed of 500 rpm at 70°C. Throughout immersing, H<sub>2</sub>O<sub>2</sub> reacted with the Ti foil creating TiO<sub>2</sub> networked nanosheets on the scratched side of the photoanode. To further improve the crystallization of TiO<sub>2</sub> nanosheets, the Ti foil was annealed for 30 min at 450°C (Tsai et al., 2013). Figure 1 shows the preparation of Ti foil (a) the oxidized surfaces of Ti foil, (b) the sandpaper scratched surface and (c) the H<sub>2</sub>O<sub>2</sub>-treated annealed surface of Ti foil.

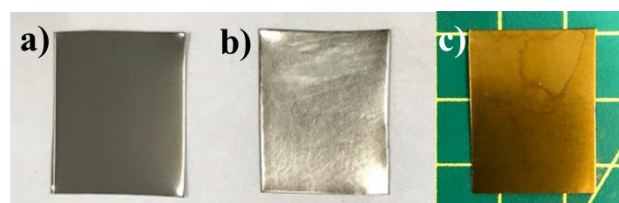


Figure 1. Preparation of Ti Foil (a) the oxidized surfaces of Ti foil, (b) the sandpaper scratched surface and (c) the H<sub>2</sub>O<sub>2</sub>-treated annealed surface of Ti foil

### D. TiO<sub>2</sub> Paste Preparation

The TiO<sub>2</sub> P25 anatase-nanopowder was preheated for 30 min in a furnace at 400°C to eliminate organic impurities and any moisture. The heated TiO<sub>2</sub> powder was mixed with 0.2ml of DI water and acetic acid respectively. The mixture was ground in a ceramic mortar. This is to lessen the particle size mean by extending the dispersion time. Also, by extending the time of grinding, the transparency of the coated film could be enhanced. This TiO<sub>2</sub> solution went through ultra-sonication at 15 min to acquire homogenous paste of TiO<sub>2</sub>. The obtained homogenous white paste was stirred at a speed of 300 rpm in room temperature for 2 hours. Then, the runny paste was evaporated at 80°C for 15 min to obtain a viscous thick paste. The paste was transferred into a bottle and sealed with parafilm to avoid any moisture adsorbed in paste (Valsaraj et al., 2016).

### E. Deposition of TiO<sub>2</sub> Layer

The TiO<sub>2</sub> paste was deposited on the Ti foil using the doctor blade method. In the experiment, 3M scotch tape was placed at the edges of the scratched Ti foil to create a  $10 \text{ mm}^2$  square area for TiO<sub>2</sub> paste deposition. Next, TiO<sub>2</sub> paste was applied on the masked top edge of Ti foil and spread across the unmasked area using a squeegee. Then, the scotch tape was removed, leaving an uncoated area of Ti foil for electrical contact for solar measurement. To evaporate the solvents and binder presented in the paste, the films were sintered at 450°C in 30 min inside the furnace. Following the cooling off to 80°C, the films were directly immersed in the red dye N719 solution dissolved with ethanol at a volume ratio of 1:1 and sealed at room temperature for a minimum of 24 hours. Figure 2 shows

(a) the sintered TiO<sub>2</sub> film on Ti foil and (b) dye-immersed Ti foil.

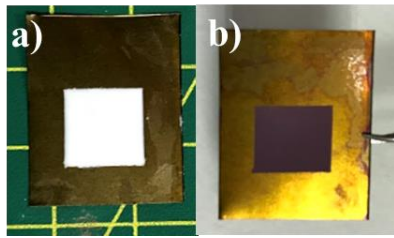


Figure 2. (a) Sintered TiO<sub>2</sub> film on Ti foil, and (b) dye-immersed Ti foil

#### F. Counter Electrode Preparation

The FTO glass was used as a counter electrode and these glasses were cleaned. To prepare the Pt solution, 2 mM of hexachloroplatinic acid was dissolved in 20 mL of isopropanol solution. Then, the solution was dropped and spin-coated on FTO glass. Next, the glass was sintered at 450°C for 30 min.

#### G. DSSC Assembly and I-V Measurement

Figure 3 (a) shows the photoanode loaded with N719 being air-dried. The fabricated counter electrodes were sandwiched together using 60 µm thick Surlyn polymer. The polymer film was cut as a spacer of 5 mm × 15 mm and framed around the area of TiO<sub>2</sub> film. Later, iodine-based electrolyte was injected into the device. Figure 3 (b) shows the solar energy conversion efficiency was tested under the solar spectrum at AM1.5 densities using a solar simulator. An evenly maintained distributed incident power densities beam homogenizer was also incorporated into the device across the irradiation area. The plotted I-V characteristic was analysed to be measured the I-V characteristic, fill factor, power output, and efficiency using Keithley 2450 SourceMeter.

#### H. Surface Morphology Characteristics

Field Emission Scanning Electron Microscopy (FESEM) was used to characterize the surface morphology of Ti Foil before and after the surface treatment of H<sub>2</sub>O<sub>2</sub>. The magnification for the characterization was 2.5 kX and 50 kX. While the Atomic Force Microscopy (AFM) used to analyze the surface

topography of the Ti foil includes the thickness and roughness of the Pt catalyst on FTO glass.

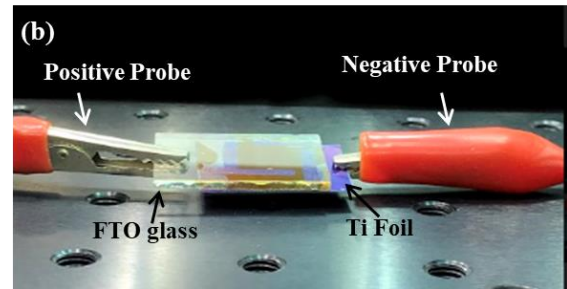
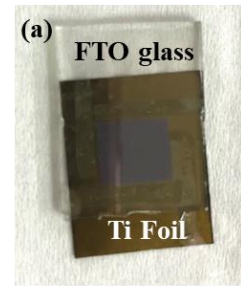


Figure 3. (a) Assembled Ti foil and Pt counter electrode and (b) setup on testing the DSSC

### III. RESULTS AND DISCUSSION

#### A. Characterization

Figure 4 shows the FESEM image of (a) Ti foil without and (b) with H<sub>2</sub>O<sub>2</sub> treatment. The untreated Ti and H<sub>2</sub>O<sub>2</sub> treated surface roughness can be seen as shown in Figure 4 (a) and (b) with the formation of packed TiO<sub>2</sub> nanosheets due to the oxidation reaction of the Ti with H<sub>2</sub>O<sub>2</sub>. The TiO<sub>2</sub> nanosheet is expected to increase the absolute area of Ti substrate because of its structure to enhance dye loading and the electrical contact between TiO<sub>2</sub> nanoparticles and the Ti substrate compared to the untreated surface. Surface morphology of the treated Ti Foil with H<sub>2</sub>O<sub>2</sub> shows the formation of TiO<sub>2</sub> nanostructure which results in significant attachment of TiO<sub>2</sub> layer on Ti Foil. (Kapil *et al.*, 2014; Tsai *et al.*, 2013).

Figure 5 (a) shows the atomic force microscopy (AFM) image of Pt-based counter electrode to measure the thickness of Pt catalyst layer. The thickness of Pt layer on FTO glass is important for back illumination due to a thicker layer can cause light reflection and reduce light transmission to the photoanode electrode (Mohammadpour *et al.*, 2015). The thickness of Pt was

measured to be approximately 3.11 nm.

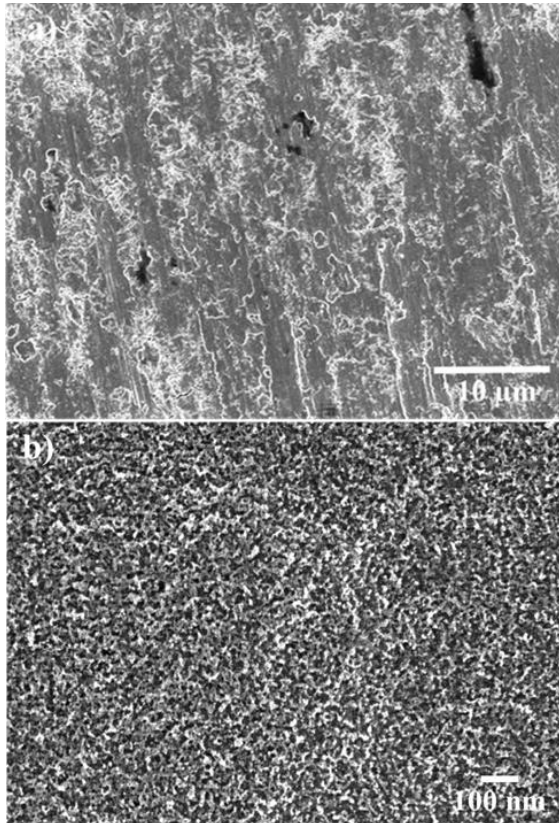


Figure 4: The Field Emission Scanning Electron Microscopy (FESEM) image of (a) Ti foil without H<sub>2</sub>O<sub>2</sub> treatment at a magnification of 2.5 kX and (b) Ti foil with H<sub>2</sub>O<sub>2</sub> treatment at a magnification of 50 kX

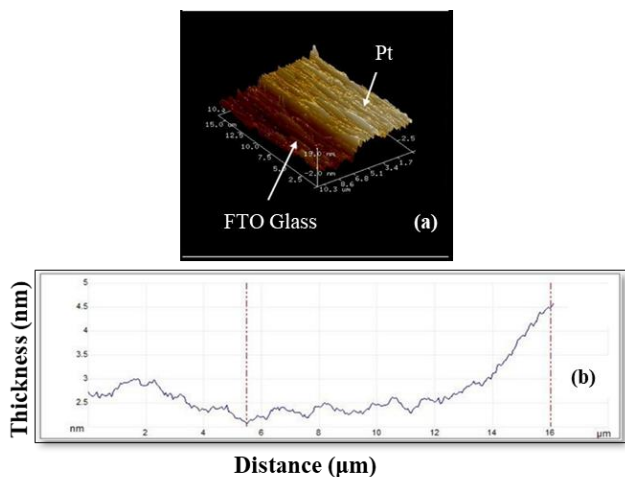


Figure 5. AFM of Pt-based counter electrode (a) 3D image and (b) thickness measurement

### B. I-V Characteristic Performance

The investigation of fabricated Ti foil flexible photoanode is performed together with the glass solid-state photoanode with

both illumination condition setup. Figure 6 shows I–V characteristics of Ti foil flexible photoanode DSSC in comparison with solid-state glass photoanode DSSC. From the plotted graph, the back-illuminated DSSC with flexible photoanode has better performance on short circuit current density, ( $J_{sc}$ ), open-circuit voltage ( $V_{oc}$ ) and the fill factor (FF), compared to glass-based DSSC. Despite that, the performance of glass-based DSSC through front illumination is highly considerable too. The transparency effect on the counter electrode gave impact to the DSSC performance (Balasingam *et al.*, 2013). The Pt and FTO layers on counter electrode reduced the transparency of the substrate. The only alternative for measurement are back-illumination hence the metal Ti photoanode based DSSC is opaque and no light can pass through with the front-illumination setup. To strengthen the performance, counter electrode transparency needs to be enhanced.

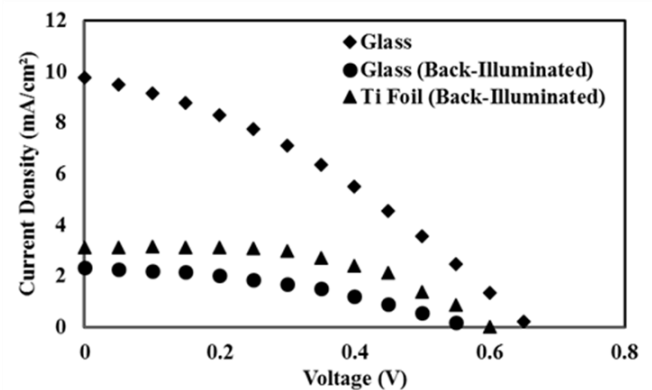


Figure 6: I-V characteristics measured (♦) the glass (front-illuminated), (●) the glass (Back-illuminated) and (▲) the Ti foil (Back-illuminated). The irradiation of solar simulator was AM 1.5 (100 mW/cm<sup>2</sup>).

Table 1 shows the performance details on DSSC with fabricated Ti foil photoanode. The measured  $V_{oc}$ ,  $J_{sc}$ , FF, and also efficiency respectively are 0.6 V, 3.12 mA/cm<sup>2</sup>, 0.51 and 1.00%,. The contrast of efficiency from back-illuminated glass DSSC reduced by half with the Ti foil DSSC and front-illuminated glass DSSC doubled with the Ti foil DSSC.

The notable drawback of this DSSC configuration is due to the losses of transmission of coated Pt at the counter electrode as well as the absorption by redox mediator electrolyte  $I^-/I_3^-$  (Jin *et al.*, 2017). The incident light was

cut by electrolyte at the back illumination slightly

Table 1: Details of DSSC Performance for front and back illumination

Parameter	Glass		Ti Foil
	Front	Back	Back
$V_{oc}$ (V)	0.65	0.55	0.60
$J_{sc}$ (mA/cm <sup>2</sup> )	9.77	2.32	3.12
Fill Factor	0.35	0.41	0.51
Efficiency (%)	2.22	0.53	1.00

from optical wavelength of 400 nm to 600 nm on Ti foil flexible photoanode DSSC while the absorbance of Pt is 540 nm to 680 nm (Ito *et al.*, 2006). The nanotube array DSSC exhibit consistently huge amount of  $V_{oc}$  typically 0.8 V incomparable to published values of 0.84V for front-illumination solar cell because of this limitation (Paulose *et al.*, 2006)

As reported in (Tsai *et al.*, 2013), the improvement of dye-loading also provides good absorption for the Ti foil photocurrent after the treatment of H<sub>2</sub>O<sub>2</sub> networked with TiO<sub>2</sub>. The method generated from this paper was applying the method of screenprint rather than the method of doctor-blade. The method of doctor-blade is not preferable for the flexible substrate as it causes rupture during fabrication due to any curvature during fabrication which disengage it from the surface as a high density of paste is applied in the doctor-blade method. Some proposals for efficiency performance at back-side illumination are displacing the electrode with an

extra translucent material. Varieties of Platinum catalyst thickness and solid-state electrolyte film could be implemented.

## IV. CONCLUSION

The surface treatment for Ti Foil with H<sub>2</sub>O<sub>2</sub> improves the surface bonding between TiO<sub>2</sub> and Ti Foil. Titanium foil as flexible photoanode has been successfully assembled and measured by back-illumination under AM 1.5. The reassuring efficiency results at 1.00% with the setup for back-illumination testing. Loss of transmission due to Pt and  $I^-/I_3^-$  electrolyte is the main drawbacks for back-illumination configuration as the iodine electrolyte cuts the incident light from 400 nm to 600 nm while the absorbance of Pt is 540 nm to 680 nm. The shorter wavelength in solar spectrum sight was the reason for the lesser efficiency of the back-illuminated measurement.

## V. ACKNOWLEDGEMENT

The authors are obliged to acknowledge the use of services and facilities of the Institute of Advanced Technology (ITMA), Universiti Putra Malaysia (UPM). Also, Malaysia-Japan International Institute of Technology (MJIT), Universiti Teknologi Malaysia (UTM). The grant (UPM/800-3/3/1/9629800) is completely supported by Universiti Putra Malaysia (UPM).

## VI. REFERENCES

- Balasingam, S K, Kang, MG, & Jun, Y 2013, Metal substrate based electrodes for flexible dye-sensitized solar cells: fabrication methods, progress and challenges, *Chemical Communications*, vol. 49, no. 98, pp. 11457-11475.
- Buda, S, Shafie, S Rashid, SA, Jaafar, H & Sharif, NFM 2017, Enhanced visible light absorption and reduced charge recombination in AgNP plasmonic photo-electrochemical cell, *Results in Physics* vol. 7, pp. 2311-2316.
- Buda, S, Shafie, S, Rashid, SA, Jaafar, H, & Khalifa, A 2017. Response surface modeling of photogenerated charge collection of silver-based plasmonic dye-sensitized solar cell using central composite design experiments, *Results in Physics* vol. 7, pp. 493-497.
- Cavallo, C, Di Pascasio, F, Latini, A, Bonomo, M & Dini, D 2017, Nanostructured semiconductor materials for dye-sensitized solar cells, *Journal of Nanomaterials*, vol. 2017.

- Conibeer, G, Green, M, Corkish, R, Cho, Y, Cho, EC, Jiang, CW & Trupke, T 2006. Silicon nanostructures for third generation photovoltaic solar cells, *Thin Solid Films*, vol. 511, pp. 654-662.
- Ellabban, O, Abu-Rub, H & Blaabjerg, F 2014. Renewable energy resources: Current status, future prospects and their enabling technology, *Renewable and Sustainable Energy Reviews*, vol. 39, pp. 748-764.
- Fan, K, Li, R, Chen, J, Shi, W & Peng, T 2013. Recent development of dye-sensitized solar cells based on flexible substrates, *Science of Advanced Materials*, vol. 5, no. 11, pp. 1596-1626.
- Ferekides, C & Britt, J 1994, CdTe solar cells with efficiencies over 15%, *Solar Energy Materials and Solar Cells*, vol. 35, pp. 255-262.
- Fthenakis, VM, Morris, SC, Moskowitz, P & Morgan, DL 1999, Toxicity of cadmium telluride, copper indium diselenide, and coppergallium diselenide, *Progress in Photovoltaics: Research and Applications*, vol. 7, no. 6, pp. 489-497.
- Gu, P, Yang, D, Zhu, X, Sun, H, Wangyang, P, Li, J & Tian, H 2017, Influence of electrolyte proportion on the performance of dye-sensitized solar cells, *AIP Advances*, vol. 7, no. 10, pp. 105219.
- Ito, S, Rothenberger, G, Liska, P, Comte, P, Zakeeruddin, SM, Péchy, P & Grätzel, M 2006. High-efficiency (7.2%) flexible dye-sensitized solar cells with Ti-metal substrate for nanocrystalline-TiO<sub>2</sub> photoanode, *Chemical Communications*, vol. 38, pp. 4004-4006.
- Jin, S, Shin, E, & Hong, J 2017, TiO<sub>2</sub> Nanowire Networks Prepared by Titanium Corrosion and Their Application to Bendable Dye-Sensitized Solar Cells, *Nanomaterials*, vol. 7, no. 10, pp. 315.
- Kapil, G, Pandey, SS, Ogomi, Y, Ma, T & Hayase, S 2014. Titanium wire engineering and its effect on the performance of coil type cylindrical dye-sensitized solar cells, *Organic Electronics*, vol. 15, no. 11, pp. 3399-3405.
- Kranz, L, Abate, A, Feurer, T, Fu, F, Avancini, E, Löckinger, J & Tiwari, A N 2015. High-efficiency polycrystalline thi film tandem solar cells, *The Journal Of Physical Chemistry Letters*, vol. 6, no. 14, pp. 2676-2681.
- Lin, LY, Lee, CP, Vittal, R & Ho, KC 2010, Selective conditions for the fabricatio of a flexible dye-sensitized solar cell with Ti/TiO<sub>2</sub> photoanode, *Journal of Power Sources*, vol. 195, no. 13, pp. 4344-4349.
- Mohammadpour, F, Moradi, M, Lee, K, Cha, G, So, S, Kahnt, A & Schmuki, P 2015. Enhanced performance of dye sensitized solar cells based on TiO<sub>2</sub> nanotube membranes using an optimize annealing profile, *Chemical Communications*, vol. 51, no. 9, pp. 1631-1634.
- Paulose, M, Shankar, K, Varghese, OK, Mor, G K, Hardin, B & Grimes, CA 2006, Backside illuminated dye-sensitized solar cells based on titania nanotube arrayelectrodes, *Nanotechnology*, vol. 17, no. 5, pp. 1446.
- Sharma, S, Jain, KK & Sharma, A 2015, Solar cells: in research and applications—A review, *Materials Sciences and Applications*, vol. 6, no. 12, pp. 1145.
- Tsai, TY, Chen, CM, Cherng, SJ, & Suen, SY 2013, An efficient titanium-based photoanode for dye-sensitized solar cell under back-side illumination, *Progress in Photovoltaics: Research and Applications*, vol. 21, no. 2, pp. 226-231.
- Tsekouras, G, Mozer, AJ & Wallace, GG 2008, Enhanced performance of dye sensitized solar cells utilizing platinum electro deposit counter electrodes, *Journal of the Electrochemical Society*, vol. 155, no. 7, pp. 124-128.
- Valsaraj, D, Subramaniam, MR, Baiju, G & Kumaresan, D 2016, Effect of organic binders of TiO<sub>2</sub> pastes in the photoanodes of cost-effective dye sensitized solar cells fabrication, *Austin ChemEng* vol. 3, no. 5.
- Wu, J, Lan, Z, Lin, J, Huang, M, Huang, Y, Fan, L & Wei, Y 2017, Counter electrodes in dye-sensitized solar cells, *Chemical Society Reviews*, vol. 46, no. 19, pp. 5975-6023.